Impact of Flexible Operation on Resilience and Reliability in Multi-Carrier Grid

Maziyar Balali Moghadam, Ahmad Ghaderi Shamim*, Farhad Samaei

Department of Electrical Engineering, Hamedan branch, Islamic Azad University, Hamedan, Iran. Email: a.ghaderi@iauh.ac.ir

Abstract

Due to the increasing need for various types of energy carriers and clean energy, the importance of exploiting and using renewable resources increases. This article aims to have a multi-carrier micro-network that can be resilient against major incidents and has adequate reliability. To achieve these goals, flexible operation of the grid under investigation is done. Then, the new reliability parameters are checked, and the resilience of the multi-carrier network with variable risk coefficients is checked in a short period of 24 hours. The investigated multi-carrier network has electricity and gas energy input. And it has electricity and heat at the output. The multi-carrier network consists of transformers, CHP, electrical and thermal storage and PHEVs. The results indicate the proper operation and reliability improvement as well as maintaining the resilience of the network in dealing with high-risk incidents. Also, the network has been able to perform well for incidents with medium risk.

Keywords: flexible operation, reliability, multicarrier micro grid- resilience
Article history: Received 2025/01/10, Revised 2025/03/20; Accepted 2025/06/05, Article Type: Research paper

1. Introduction

Today's world is a world of looming energy problems. The level of concern about existing and forthcoming energy issues is reflected in the number of international conferences and conventions dedicated to this topic. Over the years, researchers have proposed a wide variety of scientific and engineering solutions for solving or at least alleviating these issues. The crux of all energy issues is humanity's total reliance on fossil fuels, which, in addition to causing major environmental problems, will inevitably run out some time in the future. With the advancement of energy generation and conversion technologies (e.g. simultaneous generation of electricity, heat, fuel cells, etc.), recent decades have seen the emergence of new approaches in the field of energy generation, distribution, and consumption management, which can potentially offer viable solutions for alleviating the world's energy issues [1]. During these years, a number of relatively novel concepts have also emerged in the domain of power systems to improve energy distribution and consumption and address some of the aforementioned issues. The concepts of micro grid, smart grid, energy hub, reliability, and flexibility fall into this category. Efficient energy utilization is crucial for the sustainability and stability of energy systems. With increasing interest in the use of various types of energy together and therefore the reliability, efficiency, and economic viability of energy systems that make this possible, the concept of multicarrier energy network has been introduced to represent such systems. A multicarrier energy network is a system that works with multiple types of energy carriers such as electricity, natural gas, and heat. This concept can also be described as a system of energy hubs interconnected by a series of grids, where the energy produced by generators is transmitted via grids to energy hubs that use or store it after conversion [2]. In the restructuring of power grids, it is common to place generators near demand points to improve the reliability of electricity supply, especially for sensitive loads, by ensuring that in the event of major damage in the national power grid (e.g. by natural disasters, equipment failures, terrorist attacks, etc.), local generators can supply electricity to their own area, preventing blackouts. Reliability-oriented design and operating conditions of multicarrier energy networks become more important when energy carriers are not priced evenly across time slots (e.g. different hours of the day),

making it cheaper for consumers to switch between carriers depending on the time. In such a network, the consumer of a particular carrier during certain hours may even become the producer of that carrier during other hours. This adds to the complexity of these systems, making it more difficult to optimize their performance.

A) Literature review

In the past, different energy networks like electricity and natural gas used to be planned and implemented independently from each other [3]. However, the increasing use of distributed energy resources in power networks and rising concerns about the poor operation and coordination of these resources created some incentive to make sure different energy networks are well coordinated [4]. In recent years, many studies have been conducted on the world's energy outlooks given the existing management systems with their current structures and limitations. These studies have found that for better management of energy resources, different energy platforms should be merged into integrated systems, as it makes sense economically to not handle different energy carriers separate from each other. These insights have given birth to the concept of multicarrier energy system [5]. In a 2002 project on the same subject at the University of Zurich, the analyses of existing energy structures and the forecasts made for the next 50 years showed that the simultaneous use of multiple energy sources in the framework of energy hubs can offer new opportunities for better energy management, but energy hub as an emerging concept requires a new structure and formulation whereby different carriers can be handled in a coordinated manner. In [6], the energy hub was modeled as a node of the power distribution network that receives gas, electricity, and wind as input and supplies a specific load as output after carrying out conversion, storage, or load-shifting operations. The objective function of this model was formulated as the optimal operation of the energy hub in terms of economic, environmental, energy efficiency, and reliability criteria. Given the uncertainty in inputs like wind and electric load and also the real-time pricing (RTP) of energy, this model was solved with stochastic methods. In other words, this work considered the effect of the presence of distributed energy resources and the uncertainties in wind, electric load, and RTP on the operating cost and reliability of the energy hub.

B) Innovation

Considering the studies reviewed in the previous section, there is a gap in the literature in relation to how to improve the resilience and reliability of electricity distribution networks so that they can respond to different varieties of events with enough resilience and flexible reliability. In this paper, the goal is to use resilience and reliability in a multi-carrier micro grid. First, the operation of the multi-carrier micro grid in a short period of time is done in order to improve resilience, and in the next step, the reliability parameters of a multi-national micro grid that is also resilient are calculated.

At the first level, the operation is carried out in such a way as to improve the resilience of the energy hub.so that when an event occurs for the energy hub, the energy hub is connect to main grid and the operation is carried out to supply 10% of the load using the demand side management (CPP). At this level, operation is considered for a short period (24 hours). To improve the resilience and prevent the blackout of the multi-carrier micro grid, 10% of the micro grid loads are provided. The second level is the optimization of reliability parameters with a genetic algorithm. It is expected that the combination of these two levels will facilitate the selection of the best components and the best operating conditions for managing the energy hub to improve the Subscriber welfare. The main contributions of this paper are as follows:

Improving the flexible operation of the energy hub by using a new load response model that links the energy purchase price of the responsive loads to the market price of energy, purchase size, and domestic generation.

Improving system resiliency using load shedding potential as virtual production.

C) Article organization

This article is organized into five sections. The first section provides an introduction to the subject and a review of the relevant literature and then explains the innovations made in the research. The second section presents the proposed model and explains its mathematical formulations. The third section provides a method for solving the model. The fourth section discusses the details and results of a simulation conducted to evaluate the method. The fifth and final section is dedicated to presenting the conclusions.

2. Model

Figure 1 shows a conceptual model of how the problem is formulated and solved divided by stages. The considered hypothetical network is illustrated in Figure 3. Micro grid is defined as a group of loads and distributed generators in the distribution network that can act as an independent part of the national network. Micro grids can operate in two modes: 1- on-grid, which is how they normally work, and 2- off-grid (or island), which activates when the system encounters a critical fault. The subject of this article is a multicarrier micro grid

model in which the operating costs and the cost of energy not supplied are taken into account. The goal of this article is to improve the on-grid operation of this multicarrier micro grid such that its flexible reliability is also improved. For this purpose, the paper considers the multicarrier micro grid shown in Figure 2.

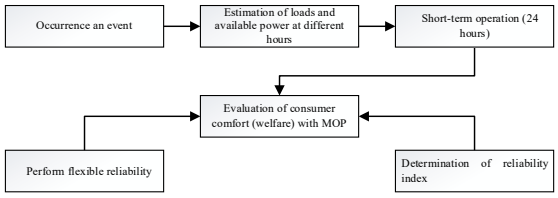

Fig. 1. Conceptual model of the problem-solving process

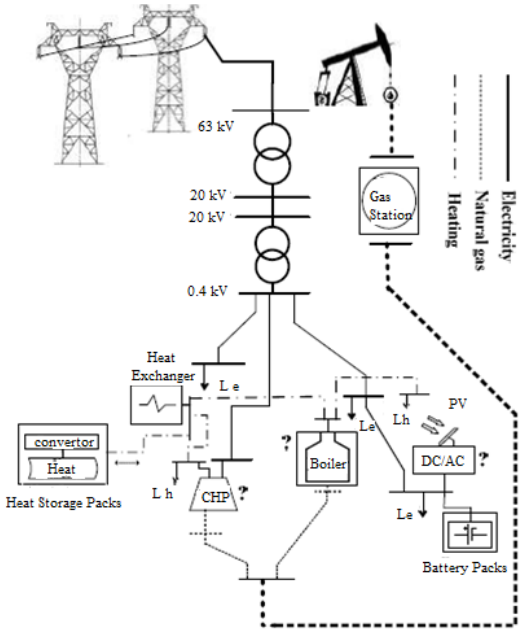

Fig. 2. An overview of the considered multicarrier micro grid

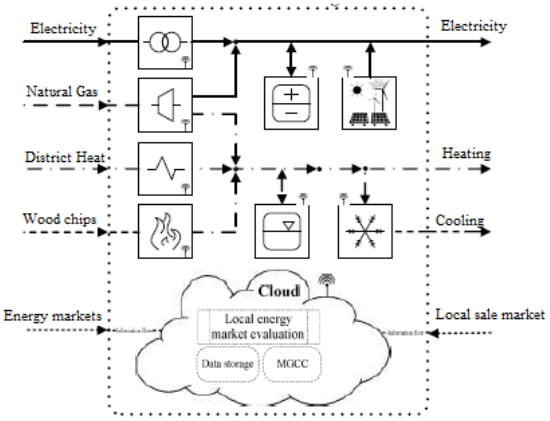

Fig. 3. Simplified structure of the considered multicarrier micro grid

This article makes use of the concept of multicarrier network as an energy hub [14]. A multicarrier network as an energy hub (multicarrier micro grid) with its input and output ports is shown in Figure 3. The location of storage systems, optimization of generators, load distribution and fault recovery analyses, etc., are performed by a controller module based on the cloud computing architecture, which here is called the central controller. This central controller is capable of monitoring distributed generation in a virtual environment, which reduces resource management and location costs.

D) Network modeling

In this article, the energy hub is modeled based on the energy network model. The electrical and thermal load balance is modeled based on the included elements using Equations (1) and (2).

$$L_e(y,m,d,t) + D_e(y.m.d.t) + T_e(y,m,d,t) = Po_e^{chp}(y,m,d,t) + Po_e^{trans}(y,m,d,t) + Po_e^{PV}(y,m,d,t) - M_e(y,m,d,t) \quad (1)$$

$$L_h(y,m,d,t) + D_h(y.m.d.t) + T_h(y,m,d,t) = Po_h^{chp}(y,m,d,t) + Po_h^{bo}(y,m,d,t) - M_h(y,m,d,t) \quad (2)$$

E) Storage modeling

The equivalent power distribution in Equations (3) and (4), which is directly related to the derivative of the energy, is formulated as follows:

$$M_l(y,m,d,t) = S_l(y,m,d,t) * \dot{E}_l(y,m,d,t) \quad (3)$$

$$M\_l\ (y,m,d,t) = ((E\_l\ (y,m,d,t) - E\_l\ (y,m,d,t-1) - E\_(l,stb)\ )) * (\ 〚Ie〛\_l\hat{}ESS\ (y,m,d,t) * \eta\_l\hat{}char - (1 - 〚Ie〛\_l\hat{}ESS\ (y.m.d.t) * \eta\_l\hat{}dischar) \quad (4)$$

To increase storage performance, storage systems are considered to have equal energy levels at the beginning and end of each planning period.

$$E_l(y,m,d,1) = E_l(y,m,d,24) \quad (5)$$

F) Responsive load modeling

Since non-responsive loads can cause major peaks (particularly in times when the energy price is lower), the concerns about such peaks are alleviated by considering responsive loads as Equation (6). The electrical and thermal responsive loads are modeled as follows.

$$D\_l\ (y,m,d,t) = D\_(0,l)\ (y,m,d,t) * (1 + e\_\alpha\ (t,t')\ .(\rho\_\alpha 0\ (t) - \rho\_\alpha 0\ (t'))/(\rho\_\alpha 0\ (t))\ ) + D\_(0,l)\ (y,m,d,t) * (1 + (\sum\_(t' \neq t)\ 〚\ 〚EL〛\_l\ (y,m,d,t,t')\ * (\rho\_l\ (y,m,d,(t))')/(\rho\_(0,l)\ (y,m,d,(t))') - (\rho\_(0,l)\ (y,m,d,t))/(\rho\_(0,l)\ (y,m,d,(t))')\ )) \quad (6)$$

G) Reliability assessment

In this article, several prominent reliability indicators are used to analyze the microgrid's reliability in meeting different demands in the on-grid mode. Specifically, the study uses the Cost of Energy Not Supplied (CENS), Energy Index of Reliability (EIR), Loss of Load Expectation (LOLE), and Loss of Load Probability (LOLP) as reliability indicators for electrical and thermal loads. Used as a measure of the damage caused by energy problems, CENS is modeled as follows.

$$EENS\rangle\_l\,(y) = \sum\_(m = 1)\^12 \sum\_(d = 1)\^30 \langle\sum\_(t = 1)\^24 \langle Pr\rangle\_(l,t) * \langle ENS\rangle\_(l,t) \quad (7)$$

The annual EIR is obtained as follows:

$$EIR\rangle\_l\^pu\,(y) = 1 - (\langle EENS\rangle\_l\,(y))/(\langle EnD\rangle\_(tot,l)(y)) \quad (8)$$

LOLE, which represents the expected hours per year in which not enough energy is supplied, is obtained from Equation (9).

$$\langle LOLE\rangle\_l\,(y) = \sum\_(m = 1)\^12 \sum\_(d = 1)\^30 \langle\sum\_(t = 1)\^24 \langle Pr\rangle\_(l,t) * \hat{t}\_(l,t) \quad (9)$$

The system failure probability is formulated as follows.

$$\langle LOLP\rangle\_l\,(y) = \sum\_(m = 1)\^12 \sum\_(d = 1)\^30 \langle\sum\_(t = 1)\^24 \langle Pr\rangle\_(l,t) \quad (10)$$

H) Objective function and constraints

Multicarrier microgrid configuration is a multi-objective problem with the objective of minimizing gross investment costs, fuel costs, maintenance costs, and loss-of-load costs for electrical and thermal loads.

$$Min: OF = C_{inv} + C_{oper} + C_{main} + \sum_{l\in(e,h)} C_{EIC,l} \quad (11)$$

The investment cost of the components (CHP generator, transformer, heat generator, and solar unit) is modeled in Equation (12). The gross costs of buying and selling energy from the network in the planning horizon are formulated in the first and second terms of Equation (13). The gross cost of equipment maintenance is computed in Equation (14) and the gross cost of loss of electrical and thermal load is obtained by multiplying the amount of energy not supplied by CENS in Equation (15).

$$C_{inv} = \left(\sum_{c=1}^{Nc^{chp}} Invs^{chp}(c) * I^{chp}(c)\right) + \left(\sum_{c=1}^{Nc^{trans}} Invs^{trans}(c) * I^{trans}(c)\right) + \left(\sum_{c=1}^{Nc^{bo}} Invs^{bo}(c) * I^{bo}(c)\right) + \left(\sum_{c=1}^{Nc^{PV}} Invs^{PV}(c) * I^{PV}(c)\right) \quad (12)$$

$$C_{oper} = \left(\sum_{y=1}^{Ny} \frac{1}{(1+i)^{y-1}}\right) * \sum_{m=1}^{12}\sum_{d=1}^{30}\sum_{t=1}^{24} \left[\begin{array}{l} + \sum_{p\in(e,g)} P_p(y,m,d,t) * \pi_p(y,m,d,t) \\ - \sum_{l\in(e,h)} T_l(y,m,d,t) * \psi_l(y,m,d,t) \end{array}\right] \quad (13)$$

$$C_{main} = \left(\sum_{y=1}^{Ny} \frac{1}{(1+i)^{y-1}}\right) * \sum_{m=1}^{12}\sum_{d=1}^{30}\sum_{t=1}^{24} \left(\sum_{c=1}^{Nc^{chp}} Po_e^{chp}(y,m,d,t) * K_{main}^{chp}(c) * I^{chp}(c) + \sum_{c=1}^{Nc^{bo}} Po_e^{bo}(y,m,d,t) * K_{main}^{bo}(c) * I^{bo}(c) + \sum_{c=1}^{Nc^{trans}} Po_e^{trans}(y,m,d,t) * K_{main}^{trans}(c) * I^{trans}(c) + \sum_{c=1}^{Nc^{PV}} Po_e^{PV}(y,m,d,t) * K_{main}^{PV}(c) * I^{PV}(c)\right) \quad (14)$$

$$C_{EIC,l} = VOLL_l * \sum_{y=1}^{Ny} \frac{EENS_l(y)}{(1+i)^{y-1}} \quad (15)$$

The energy generation of the CHP unit, transformer, heat generator, and solar unit is modeled by the following equations.

$$Po_l^{chp}(y,m,d,t) = \sum_{c=1}^{Nc^{chp}} P_g(y,m,d,t) * \eta_l^{chp}(c) * v^{chp}(t.m) * I^{chp}(c),\ l \in \{e,h\} \quad (16)$$

$$Po_e^{trans}(y,m,d,t) = \sum_{c=1}^{Nc^{trans}} P_e(y,m,d,t) * \eta_e^{trans}(c) * I^{trans}(c) \quad (17)$$

$$Po_h^{bo}(y,m,d,t) = \sum_{c=1}^{Nc^{bo}} P_g(y,m,d,t) * \eta_l^{bo}(c) * v^{bo}(t.m) * I^{bo}(c) \quad (18)$$

$$Po_e^{PV}(y,m,d,t) = \sum_{c=1}^{Nc^{PV}} RP_e^{PV}(y,m,d,t) * \eta_e^{PV}(c) * I^{PV}(c) \quad (19)$$

The minimum and maximum operating limits of the CHP unit, transformer, heat generator, and solar unit are formulated below.

$$\sum_{c=1}^{Nc^{chp}} \underline{Po_e^{chp}(y,m,d,t)} . I^{chp}(c) \le Po_e^{chp}(y,m,d,t) \le \sum_{c=1}^{Nc^{chp}} \overline{Po_e^{chp}(y,m,d,t)} . I^{chp}(c) \quad (20)$$

$$\sum_{c=1}^{Nc^{trans}} \underline{Po_e^{trans}(y,m,d,t)} . I^{trans}(c) \le Po_e^{trans}(y,m,d,t) \le \sum_{c=1}^{Nc^{trans}} \overline{Po_e^{trans}(y,m,d,t)} . I^{trans}(c) \quad (21)$$

$$\sum_{c=1}^{Nc^{bo}} \underline{Po_h^{bo}(y,m,d,t)} . I^{bo}(c) \le Po_h^{bo}(y,m,d,t) \le \sum_{c=1}^{Nc^{bo}} \overline{Po_h^{bo}(y,m,d,t)} . I^{bo}(c) \quad (22)$$

$$\sum_{c=1}^{Nc^{PV}} \underline{Po_e^{PV}(y,m,d,t)} . I^{PV}(c) \le Po_e^{PV}(y,m,d,t) \le \sum_{c=1}^{Nc^{PV}} \overline{Po_e^{PV}(y,m,d,t)} . I^{PV}(c) \quad (23)$$

The amount of energy received and transmitted from the network is given below.

$$\underline{P_p(y,m,d,t)} \le P_p(y,m,d,t) \le \overline{P_p(y,m,d,t)} \quad (24)$$

$$\underline{T_l(y,m,d,t)} \le T_l(y,m,d,t) \le \overline{T_l(y,m,d,t)} \quad (25)$$

Constraints (26) and (27) show the energy storage capacity and the charge and discharge rate of storage units.

$$\underline{E_l(y,m,d,t)} \le E_l(y,m,d,t) \le \overline{E_l(y,m,d,t)} \quad (26)$$

$$|M_l(y,m,d,t)| \le \overline{zm_l(y,m,d,t)} \quad (27)$$

The distribution of gas input into the CHP generator and the heat generator is defined as follows.

$$v^{chp}(y,m,d,t) + v^{bo}(y,m,d,t) = 1 \quad (28)$$

LOLE and LOLP are defined as Equations (29) and (30), respectively. These values must remain lower than a certain limit over the planning period.

$$v^{chp}(y,m,d,t) + v^{bo}(y,m,d,t) = 1 \quad (29)$$

$$LOLP_l(y) \le \overline{LOLP_l^{targeted}} \quad (30)$$

I) Power distribution

DC load distribution equations for buses n and m are as follows [13]:

$$P_{nm}(t) = \frac{V_n V_m}{x_{nm}} \sin(\delta_n(t) - \delta_m(t)) \quad (31)$$

$$LOLP_l(y) \le \overline{LOLP_l^{targeted}} \quad (32)$$

$$P_e^H(t) = \sum_{n=1}^{m} B_{nm} \sin(\delta_n(t) - \delta_m(t)) \quad (33)$$

$$-line_{e,nm} \le B_{nm} \sin(\delta_n(t) - \delta_m(t)) \le line_{e,nm} \quad (34)$$

The gas load distribution equations are formulated as follows:

$$S_{gf}(t) = sign\left(\gamma_g^2(t) - \gamma_f^2(t)\right) \quad (35)$$

$$-line_{g,gf} \le S_{gf}(t) MK_{gf} \sqrt{S_{gf}(t)\left(\gamma_g^2(t) - \gamma_f^2(t)\right)} \le line_{g,gf} \quad (36)$$

J) Mathematical model of network resilience

$$OF = \sum_{\omega=1}^{\omega} \rho Max(\omega) RI(\omega) \quad (37)$$

$$\sum_{l=1}^{L} x_l C_l^H + \sum_{mg=1}^{3} x_{mg} C^{PHEVs} cap_{mg}^{PHEVs} \le B \quad (38)$$

$$RI = R_{mg1} + R_{mg2} + R_{mg3} \quad (39)$$

$$R_{mg} = SRI_1 + SRI_2 + SRI_3 \quad (40)$$

The value of each R is calculated based on the figure as shown below:

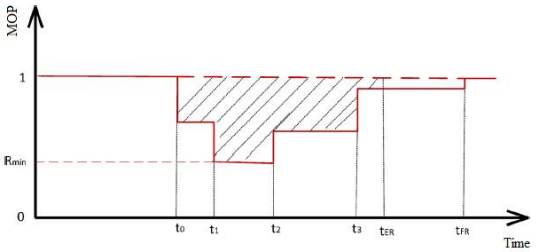

Fig. 4. Figure 4. Basic social welfare [10].

As shown in Figure 4, the moment when the event occurs and the network leaves, the normal range is assumed to be t0. In this study, considering that the medium-term operation is supposed to last one week, the full recovery time t_{FR} is considered to be 161 [10].

$$SRI_1 = R_{\min} \qquad 0 \le SRI_1 \le 1 \quad (41)$$

$$SRI_2 = \frac{\int_{t_0}^{t_{ER}} MOP\ (t)dt}{t_0 * t_{ER}} \leq SRI_2 \leq 1 \quad (42)$$

$$SRI_3 = \frac{t_{min}}{t_{FR}} \qquad 0 \leq SRI_3 \leq 1 \quad (43)$$

second objective function, which aims to minimize rearrangement time, is formulated as follows:

$$OF_2 = Max \quad MOP \quad (44)$$

$$MOP = \sum_{i=1}^{N\,load} L_i LSF_i \quad (45)$$

$$LSF_i = \begin{cases} 1 & if\ load\ is\ connected \\ 0 & if\ load\ is\ disconected \end{cases} \quad (46)$$

3. Solution method

The main goal of the proposed model is to improve the operating conditions of the energy hub and minimize the objective function without violating reliability constraints. The solution algorithm (based on the relevant reliability indicators) is shown in Figure 5. The procedure starts with processing the input parameters to produce the energy hub's initial data. In this stage, to reduce the costs arising from energy hub reliability improvement, first, flexible operation configuration is performed with RTP demand-side management and the amount of energy required for storage and exchange with the upstream network is determined on a daily basis. Then, reliability parameters are modeled and optimized with a GA that is optimized with ICA. The algorithm then determines and evaluates the value of the fitness function for each chromosome (system components and their specifications). Whenever the obtained fitness value exceeds the defined reliability limit, a penalty is applied to the function.

4. Simulation and numerical results

In this section, the proposed method is discussed in two levels: 1- flexible operation configuration of the multicarrier micro grid with the objective of minimizing costs and optimizing supply; 2- improving the reliability parameters of the network. The design of the multicarrier micro grid in the on-grid mode is displayed in Figure 2. As can be seen, this multicarrier micro grid is connected to the local electricity, gas, and heating network. The supply-demand balance is maintained by distributed energy sources and the external network. It is assumed that five types of each component (transformer, CHP unit, heat generator, and solar unit) are available for use in the network. The specifications of the system components and storage units are given in Table 1 and Table 2. Micro grid modeling is done for 5 years based on gross cost with interest rate. Installation operations are assumed to be limited to the first year of planning. In the first level, Short-term operation is done to improve resilience. Table 3 shows the economic factors assumed for the problem. The assumed market energy price is shown in Figure 6. As this figure shows, heat is assumed to have a purchase price of 0.08 \$/kWh and a selling price of 0.042 \$/kWh. The purchase and selling price of electric energy is considered to be 0.04 \$/kWh during hours 1-7, 0.05 \$/kWh during hours 8-18, and 0.08 \$/kWh during hours 19-22. The purchase price of gas is assumed to be 0.045 \$/m^3. The operating cost of DG and auxiliary heat generator is considered to be 0.04 \$/kWh and 0.033 \$/kWh, respectively. The operating cost of CHP in energy hub is 0.045. for responsive electrical and thermal loads is assumed to be three times the market price of energy. It should be mentioned that using the load response technique decreases the size of peaks as well as network costs, and using storage units prevents energy wastage in the network. Figure 7 shows the amount of heat and electricity consumed for a day. The electrical and thermal responsive loads are given in Figure 8, which shows how these loads can be changed to reduce the system's operating cost. Demand elasticity for electrical and thermal energy is given in Table 4. B (susceptance) is 10 for every energy hub and MK (gas flow rate) for hub and main grid is 4, 3 respectively. The electric energy balance of a hub for a day is shown in Figure 9. This hub buys energy from the upstream network during hours 1, 2, 11, 12, and 24 when electricity is cheaper and sells energy to the network during hours 16, 22, and 23 hours when electricity is more expensive. The outputs of DG and CHP units reach their maximum level at hour 16 when demand is extremely high. During this hour, excess power output is sold to the upstream network. At hours 22 and 23, DG and CHP units are used to meet local demand and also sell energy to the network. In this hub, electricity storage units are charged at hours 3-6 and 13 when electricity is cheaper. During these hours, DG and CHP units are used to charge electricity storage units. The charged electricity storage units are discharged at hours 7, 8, 10, 11, and 20 to meet local demand while maintaining optimal scheduling for DG and CHP units. The same hub's thermal energy balance for a day is shown in Figure 10. This hub sells thermal energy to the network during hours 1-3, 22, and 24. For this purpose, the hub uses the auxiliary heat generator as well as CHP and primary heat generator in hours 1, 2, and 22. At hour 24, only CHP and heat generator units are used to supply heat to the system, and the excess heat is sold to the network. Because of the low demand for heat during hours 6-9, the excess heat produced by CHP and heat generator units is used to charge the hub's heat storage units. These storage units are

discharged during hours 15, 18, 21, and 23 to meet the hub's local heat demand. The hub's energy load after the implementation of the RTP-based demand response program is shown in Figure 11. As can be seen, the hub manager decides to reduce the hub's energy consumption at hours 10, 11, 16, and 18-22, which results in increased energy consumption at hours 1-9 and 24. The manager of hub No.1 decides to shift the load according to market energy prices and optimal resource planning strategies. The results of thermal load management are presented in Figure 12. To evaluate the method, multicarrier micro grid modeling was performed with and without reliability indicators. The results of the solution process, including the optimal values and specifications of micro grid components are given in Table 5. In this evaluation, LOLE and LOLP were determined to be 10 hours (per year) and 0.1% (per year) respectively. As shown in Table 5, in the model where reliability is taken into account, a larger CHP generator has been chosen to ensure greater electrical and thermal outputs. In this model, the type-3 transformer has been selected because of its lower unavailability (outage), the type-4 CHP generator has been chosen for its low unavailability and its ability to supply multiple carriers simultaneously, the type-4 heat generator has been selected for its low maintenance and good efficiency in supplying part of the required thermal energy, and finally, the type-3 photovoltaic unit has been chosen because of its ability to generate electricity at negligible cost and its good capacity and efficiency considering the investment cost. In comparison, the model where reliability is ignored has chosen a cheaper CHP generator and no heat generation unit.

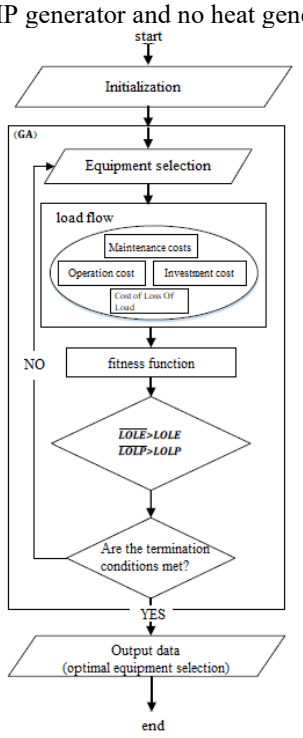

Fig. 5. Flowchart of the solution process

Table.1.
Specifications of storage units

Charge-discharge efficiency (%)	*Capacity (kWh)*	*Stored energy*
95	90	Electricity
95	90	Heat

Table.2.
Specifications of system components

Component	*Type*	*Capacity (kW)*	*Efficiency (%)*			*Installation cost (million dollars)*	*Maintenance cost factor ($/kWh)*	*Forced Outage Rate (%)*
			Electricity	*Heat*	*Total*			
Transformer	1	800	92	-	92	0.825	0.003	0.35
	2	900	90	-	90	1.328	0.0027	0.026
	3	100	89	-	89	1.66	0.0024	0.014
	4	1500	87	-	87	2.49	0.0022	0.005
	5	1800	85	-	85	2.988	0.002	0.002
CHP	1	500	40	35	75	0.221	0.015	0.02
	2	600	40	44	84	0.272	0.0135	0.05
	3	825	50	30	80	0.375	0.125	0.025
	4	1125	40	40	80	0.487	0.115	0.01
	5	1350	35	40	75	0.6	0.01	0.016
Heat generator	1	300	-	90	90	0.75	0.009	0.035
	2	450	-	87	87	0.1	0.008	0.031
	3	600	-	85	85	0.125	0.005	0.025
	4	750	-	83	83	0.15	0.003	0.02
	5	900	-	80	80	0.175	0.002	0.015
Solar unit	1	50	90	-	90	0.0625	0.0017	0.028
	2	70	88	-	88	0.087	0.0015	0.029
	3	100	85	-	85	0.125	0.0014	0.014
	4	120	82	-	82	0.15	0.0012	0.028
	5	150	80	-	80	0.187	0.001	0.036

Table.3.
Economic parameters

Annual interest rate (%)	*Annual load growth rate (%)*	*Annual growth of energy purchase cost (%)*
15	10	20

Table.4.
Demand elasticity parameter

Elasticity	*Time (h)*	*t1-t7*	*t8-t14*	*t15-t22*	*t23-t24*
Electricity	t1-t7	0	0.01	0.02	0
	t8-t14	0	-0.01	0.01	0
	t15-t22	0	0	-0.03	0
	t23-t24	0	0	0	0
Heat	t1-t7	-0.03	0	0	0
	t8-t14	0.02	0	0.02	0.02
	t15-t22	0.01	0	-0.02	0.01
	t23-t24	0	0	0	-0.03

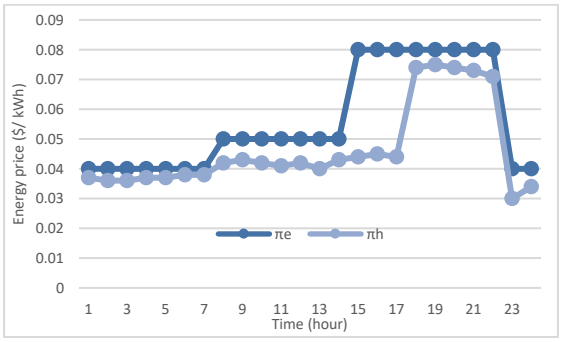

Fig. 6. Energy exchange cost for a day

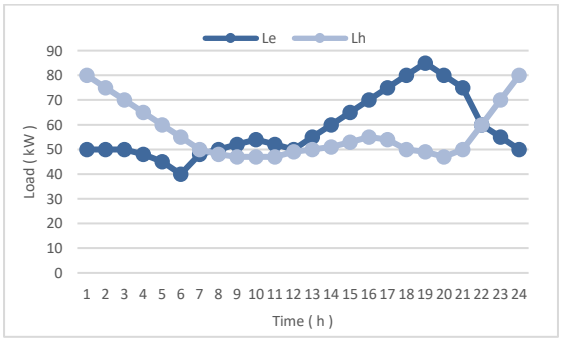

Fig. 7. 10% Electrical and thermal loads for a day

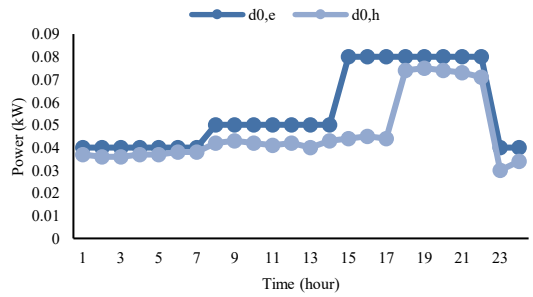

Fig. 8. Responsive electrical and thermal loads

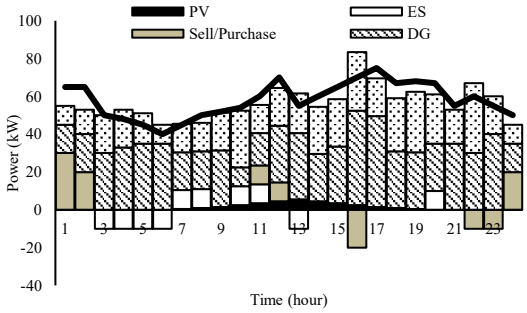

Fig. 9. Electric energy balance of the energy hub

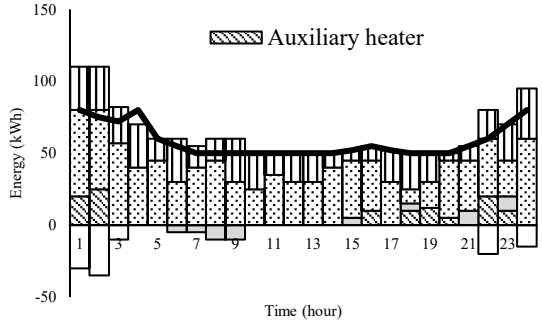

Fig. 10. Thermal energy balance of the energy hub

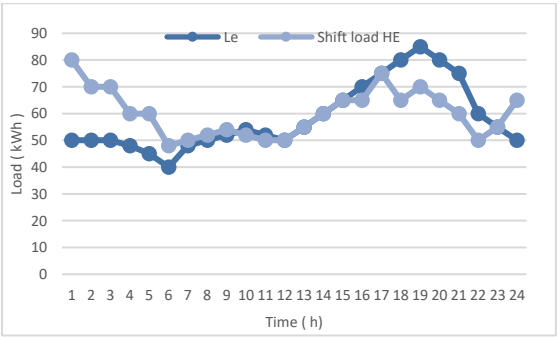

Fig. 11. Electric responsive load performance

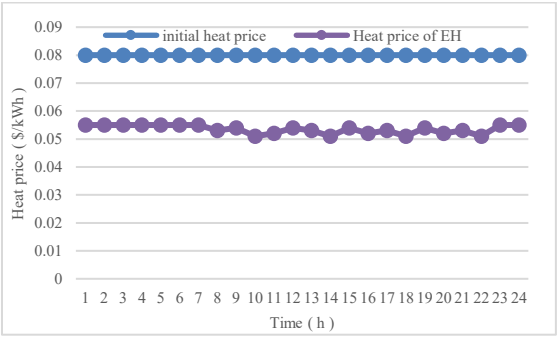

Fig. 12. Thermal responsive load performance

Table.5.
Specifications of the components chosen for the system with and without reliability consideration

Optimization approach	Components	Capacity (kW)	Efficiency (%)			Investment cost (million dollars)	Maintenance cost factor ($/kWh)	Failure rate (%)
			Electricity	Heat	Total			
With reliability consideration	Transformer 3	1000	92	-	92	1.66	0.0024	0.014
	CHP 4	1125	50	40	90	0.487	0.0115	0.01
	Heat generator 4	750	-	83	83	0.15	0.003	0.02
	Solar unit 3	100	85	-	85	0.125	0.0014	0.017
Without reliability consideration	Transformer 3	800	89	-	89	0.825	0.003	0.035
	CHP 4	825	40	30	70	0.375	0.0125	0.025
	Heat generator 4	-	-	-	-	-	-	-
	Solar unit 3	100	85	-	85	0.125	0.0014	0.014

Table.6.
Reliability indicators obtained for the system with and without reliability consideration

Results	Year	ENNS (kWh)		EIR (pu)		LOLE (Hour)		LOLP (%)	
		Electricity	Heat	Electricity	Heat	Electricity	Heat	Electricity	Heat
With reliability consideration	1	927	1577	0.9997348	0.999168	2.4192	6.9	0.028	0.08
	2	1025	1728	0.9997334	0.991709	2.4192	6.9	0.028	0.08
	3	1333	1895	0.9997322	0.991736	2.4192	6.9	0.028	0.08
	4	1251	2079	0.9997311	0.99176	2.4192	6.9	0.028	0.08
	5	1382	2280	0.9997301	0.991782	2.4192	6.9	0.028	0.08
	1-5	5719	9559	0.999732	0.99173	12.096	34.6	-	-
Without reliability consideration	1	5792	197100	0.9983426	0.8960112	15.12	863.9	0.09	0.1
	2	6402	216100	0.9983342	0.8963738	15.12	863.9	0.32	0.1
	3	7122	236900	0.9983758	0.8967035	21.489	863.9	0.5	0.1
	4	9885	259800	0.9978748	0.8970032	61.34	863.9	0.1182	0.1
	5	15250	285100	0.9970192	0.8972756	91.88	863.9	0.1182	0.1
	1-5	44450	1195000	0.9979165	0.8967332	201.95	863.9	-	-

As can be seen, considering the reliability constraints has led to significantly improved CENS. Table 7 compares the gross costs of the system over the planning period. It can be seen that reliability constraints have affected the type and size of components chosen for the multicarrier micro grid and the investment cost. It should be mentioned that considering reliability has drastically increased the overall cost of the system by restricting the options to the component that can satisfy reliability constraints. However, it also has significantly improved the system's reliability indicators.

These results demonstrate the ability of the proposed method to make sure that the demand is met with appropriate reliability. In the end, the cash flow diagram of the micro grid is drawn in Figure 11 for a better economic analysis. According to this diagram, the energy hub with reliability constraints will pay back the capital spent in its development in about four and a half years. Comparing the proposed method with the methods provided in [15] and [16] shows that it results in a 22-24% increase in investment cost by requiring the energy hubs to meet the reliability requirements. Finally, it should be mentioned that while the analysis of multicarrier micro grid design with reliability consideration may prolong the optimization process, it certainly gives the planner a better understanding of the risks associated with changes in system costs and helps achieve more reliable and realistic results from the developer's point of view. Figure 14 shows relationship between resilient in variable risk in fixed investment. According to Figure 14, it can be seen that the network has been able to perform well for medium risk incidents.

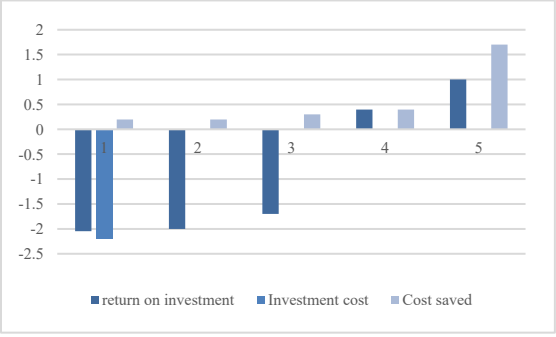

Fig. 13. Cash flow diagram of the considered multicarrier micro grid

Table.7.
Economic analysis of micro grid costs with and without reliability consideration

Results	*Year*	*Investment cost (million dollars)*				*maintenance cost (million dollars)*		*EIC in terms of net amount (million dollars)*		*Total cost (million dollars)*
		Transformer 3	*CHP 4*	*Heat generator 4*	*Solar panel 3*	*Present value*	*Net cost (NPV)*	*Electric load*	*Thermal load*	
With reliability consideration	1	-	-	-	-	0.677	0.517	0.000315	0.000283	0.3
	2	-	-	-	-	0.79	0.589	0.000303	0.000271	
	3	-	-	-	-	0.172	0.673	0.000291	0.000257	
	4	-	-	-	-	0.545	0.771	0.000279	0.000266	
	5	-	-	-	-	1.545	0.883	0.000468	0.000224	
	1-5	1.66	0.487	0.15	0.125	4.801	3.433	0.001458	0.001292	
Without reliability consideration	1	0.825	0.375	-	0.125	0286	0.486	0.001969	0.035477	0.0004
	2	-	-	-	-	0.633	0.55	0.001893	0.033816	
	3	-	-	-	-	0.829	0.426	0.001831	0.032243	
	4	-	-	-	-	1.09	0.717	0.00221	0.030752	
	5	-	-	-	-	1.44	0.822	0.002963	0.029337	
	1-5	0.825	0.375	-	0.125	4.48	3.2	0.010864	0.16145	

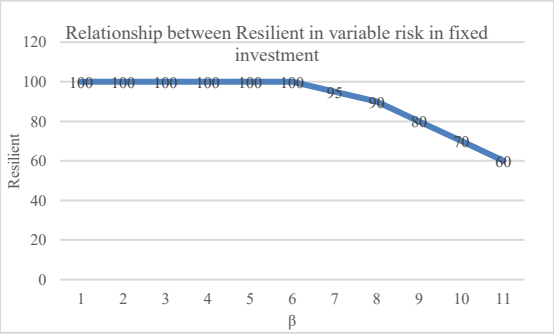

Fig. 14. Relationship between Resilient in variable risk in fixed investment

5. Conclusion

This article proposed a hybrid strategy for modeling and formulation of the design of multicarrier micro grids (energy hubs) with improve resilience and reliability Index. The proposed method involves developing a programming problem with the objective of minimizing operating and investment costs as well as the cost of energy not supplied for multiple loads. Multiple reliability indicators including the Cost of Energy Not Supplied (CENS), Energy Index of Reliability (EIR), Loss of Load Expectation (LOLE), and Loss of Load Probability (LOLP) were used in the optimization process to make sure of a reasonable level of reliability in meeting demand.

The proposed model was applied to a single-bus multicarrier micro grid to determine the optimal type and size of distributed generation components for providing uninterrupted electricity and heat supply over the planning horizon at minimum cost. The simulation results showed the great impact of considering the reliability constraints in the model on the structure and operation of the multicarrier micro grid. For example, it led to the selection of larger but also more expensive CHP generators, which, at the first glance, offers improved reliability at a prohibitively great expense. However, this level of reliability in supplying energy to various types of demand can also generate notable economic benefits over the operating horizon. The paper also provided a novel load response model that links the energy purchase price of responsive loads to the market price of energy, energy purchase size, and domestic generation. Overall, the results demonstrated the effectiveness of the proposed model in achieving the stated goals.

References

[1] Zhao, Pengfei, et al. "Economic-Effective Multi-Energy Management with Voltage Regulation Networked with Energy Hubs." IEEE Transactions on Power Systems (2020).

[2] Bostan, Alireza, et al. "Optimal scheduling of distribution systems considering multiple downward energy hubs and demand response programs." Energy 190 (2020): 116349.

[3] F. Angizeh, M. Parvania, M. Fotuhi-Firuzabad, and A. Rajabi-Ghahnavieh, " Flexibility scheduling for large customers ",IEEE Trans. Smart Grid, 2017.

[4] Kong, Tae-Sik, et al. "Study on reliability improvement of voltage transformers by increasing voltage factor." Journal of Electrical Engineering & Technology 15.3 (2020): 1463-1469.

[5] AminiKhoei, Zahra, Abbas Kargar, and Sayed Yaser Derakhshandeh. "Reactive Power Sharing Among

Distributed Generation Sources in Islanded Microgrids to Improve Voltage Stability." Smart Grids and Sustainable Energy 8.3 (2023): 15.

[6] A. Helseth and A. Hollen, “Reliablity modelling of gas and electric power distribution systems; similarities and differences”, 9th international conference on probabilistic methodsapplied to power systems, Stockholm, Sweden, 2019.

[7] G. A. Koepple, “Reliability Consideration of Future Energy Systems: Multi-Carrier Systems and the Effect of Energy Storage”, PHD Thesis, Swiss Federal Institute of Technology ETH Zurich, Switzerland, Dissertation ETH no. 17058, 2018.

[8] Gargari, Milad Zamani, and Reza Ghaffarpour. "Reliability evaluation of multi-carrier energy system with different level of demands under various weather situation." Energy 196 (2020): 117091.

[9] Chauhan, K., and R. K. Chauhan. "Optimization of grid energy using demand and source side management for DC microgrid." Journal of Renewable and Sustainable Energy 9.3 (2017).

[10] Azizi, Ali Akbar, Ahmad Ghaderi Shamim, and Mohamad Ehsan Mosayebian. "Robust island-mode operation of power distribution network using game theory for resilience enhancement." Sustainable Energy, Grids and Networks 33 (2023): 100978.

[11] C. Dai, L. Wu and H. Wu, "A Multi-Band Uncertainty Set Based Robust SCUC With Spatial and Temporal Budget Constraints," in IEEE Transactions on Power Systems, vol. 31, no. 6, pp. 4988-5000, Nov. 2016.

[12] Olivares et al. D. E, "A Centralized energy management system for isolated microgrids",IEEE Trans. Smart Grid, Vol. 5, No. 4, pp. 1864– 1875, 2014.

[13] Rahmatian, Mohammad Rasoul, Ahmad Ghaderi Shamim, and Salah Bahramara. "Optimal operation of the energy hubs in the islanded multi-carrier energy system using Cournot model." Applied Thermal Engineering 191 (2021): 116837.

[14] Amir, V., Jadid, S. and Ehsan, M., "Optimal planning of a multi-carrier microgrid (MCMG) considering demand-side management", Int. J.Renew. Energy Res, Vol. 8, No. 1, pp. 238–249,2018.

[15] Amir, V., Jadid, S. and Ehsan, M., "Optimal design of a multi-carrier microgrid (MCMG) considering net zero emission", Energies, Vol. 10, No. 12, pp. 2019–2030, 2017.

[16] C. Dai, L. Wu and H. Wu, "A Multi-Band Uncertainty Set Based Robust SCUC With Spatial and Temporal Budget Constraints," in IEEE Transactions on Power Systems, vol. 31, no. 6, pp. 4988-5000, Nov. 2016.

Nomination

y, m, d, t	Year, month, day , time
g,f	Gas bus number
n,m	Electricity bus number
P	Input carrier
R	Number of competitors
Rp	Renewable energy production
L_e	Electrical demand non-Response (kW)
L_h	Heat demand non-Response (kW)
D_e	Electrical demand Response (kW)
D_h	Heat demand Response (kW)
$D0$	Initial Responsive load (kW)
B_{mn}	Susceptance (ʊ)
b	Auxiliary heater
π	Purchase energy price ($/kWh)
ψ	Cell energy price ($/kWh)
D	Responsive load (kW)
Po_e^{trans}	The energy produced by the transformer (kWh)
Po_e^{chp}	The Electrical energy produced by the CHP kWh
Po_h^{chp}	The Heat energy produced by the CHP (kWh)
M_e	Electrical Efficiency
M_h	Heat Efficiency
T_e	Transmission of electrical energy
T_h	Transmission of Heat energy
Po_e^{PV}	The Heat energy produced by the PV (kWh)
Po_h^{bo}	The Heat energy produced by the Boiler (kWh)
M_l	Load Efficiency
S_l	Coupling factor
$\dot{E}_l$	Energy storage
$E_{l,stb}$	Wasted energy stored (kW)
Ie_l^{ESS}	Binary variable of charging and discharging status
$EENS_l(y)$	Unsupplied energy costs
η_l^{char}	Charging efficiency
$\eta_l^{dischar}$	Discharge efficiency
α	Type of energy carrier
$e_\alpha(t, \dot{t})$	The cost of purchasing an electricity carrier
$\rho_{\alpha 0}(\dot{t})$	The cost of purchasing the goods is responsible
P_g	gas carrier
η_l^{chp}	CHP Efficiency
P_g	Gas Input
P_{nm}	Active power between buses n and m (kW)
S_e	Sign function for electrical storage
S_{gf}	Sign function for gas flow between buses g and f
S_h	Sign function for heat storage
$v^{chp}(t.m)$	CHP gas distribution coefficient
$v^{bo}(t.m)$	Boiler gas distribution coefficient
V_n, V_m	Voltage of buses n , m, respectively (Volt)
$line_{e,nm}$	Electrical capacity of line connects bus n to m
$line_{g,gf}$	Gas capacity of line connects bus g to f
MK_{gf}	Pipe and fluid specifications of buses g and f
$ENS_{l,t}$	Expected unsupplied energy
$EnD_{tot,l}(y)$	Total annual energy
$EIR_l^{pu}(y)$	Reliability energy index
$LOLE_l(y)$	Waiting for load cut
$\hat{t}_{l,t}$	cut off time
$LOLP_l(y)$	Possibility of load interruption
C_{inv}	Investment cost ($)
C_{oper}	Operation cost ($)
C_{main}	Maintenance costs ($)
$Invs^{chp}(c)$	CHP Installation and investment cost ($)
$Invs^{trans}(c)$	transformer Installation and investment cost ($)
$Invs^{bo}(c)$	Boiler Installation and investment cost ($)
$Invs^{PV}(c)$	PV Installation and investment cost ($)
$I^{chp}(c)$	CHP Binary variable
$I^{trans}(c)$	transformer Binary variable
$I^{bo}(c)$	Boiler Binary variable
$I^{PV}(c)$	PV Binary variable
$K_{main}^{chp}(c)$	CHP maintenance cost factor ($)
$K_{main}^{bo}(c)$	Boiler maintenance cost factor ($)
$K_{main}^{trans}(c)$	Transformer maintenance cost factor ($)
$K_{main}^{PV}(c)$	PV maintenance cost factor
$C_{EIC,l}$	Cost of load ($/kWh)
$VOLL_l$	Cost of load shedding
$\sum_{t=1}^{24} Pr_{l,t}$	Possibility of load interruption
η_e^{trans}	Transformer electrical efficiency
$\eta_l^{bo}(c)$	Boiler thermal efficiency
$\eta_e^{PV}(c)$	PV electrical efficiency
MOP	Measurement of Performance
OF	Objective function
$L_i LSF_i$	Satisfaction function of load
SRI_1	First sub-resilience index

SRI_2	Second sub-resilience index
SRI_3	Third sub-resilience index